J Mater Sci: Mater Electron (2017) 28:14855–14863
DOI 10.1007/s10854-017-7357-9

The injection of Ag nanoparticles on surface of WO_3 thin film: enhanced electrochromic coloration efficiency and switching response

S. Hoseinzadeh[1] · R. Ghasemiasl[1] · A. Bahari[2] · A. H. Ramezani[3]

Received: 14 February 2017 / Accepted: 13 June 2017 / Published online: 26 June 2017

Abstract An electrochromic (EC) thin film based on composite of tungsten oxide and Ag nanoparticles was prepared by physical vapor deposition (PVD) method. In this method, WO_3 nanoparticles powder with uniform rate was deposited in vacuum on fluorine doped tin oxide (FTO) coated glass substrate. The Ag nanoparticles powder was utilized to decorate the surface of WO_3 thin film by using PVD method. The EC thin film was annelid to inject the Ag nanoparticles into the surface of thin film. The EC nanocomposite thin film with the approximate thickness of 315 nm and smooth surface was obtained. EC properties of WO_3–Ag thin film was investigated by cyclic voltammetry (CV) and the visible transmittance to compare the existence of Ag nanoparticles beside WO_3 nanoparticles by PVD method. Also, the optical response and coloration efficiency (CE) of samples were investigated. In particular, a significant optical modulation (39.65% at 632.8 nm) and high CE (74.2 cm^2/C at 632.8 nm) are achieved that are much better than thin film only composed of WO_3.

1 Introduction

Over the last years, the use of renewable energy sources has been growing for many different applications. However, using energy efficiently is one of the most important energy solution strategies. As an example of these strategies, using energy from sunlight through photovoltaic phenomenon is being widely demanded as a fundamental alternative of future energy solutions. But the uncontrollable and periodic natures of these alternative energy sources are encouraged the attempts to use of an efficient energy storage system. For instance, using smart windows on buildings by replacing highly glazed glass is one of the important of these attempts [1, 2].

In briefly, the smart windows can be optimized either for cooler or hotter climates or designed to give a compromise between the two extremes. The use of this technology became popular in 1980s. Such windows were widely based on electrochromism with variable transmittance of light and solar energy. Electrochromic (EC) phenomenon that companied with the double injection and extraction of electrons and ions shows a reversible and optical change due to oxidation/reduction mechanism after applying different voltages (≤3 V) [3–5]. The EC materials can be divided to three categories such as inorganic materials (transition metal oxides), single molecular materials and organic polymeric materials (π-conjugated conducting polymers) that can be used for various applications as elements of information display, automotive rear-view mirrors, smart windows and military camouflages [6–8]. Electrochemical devices (ECDs) at simplest state are formed of three layers: EC materials, electrolytes and electrodes. Extensive researchs on each of these layers are done to enhance the efficiency of ECDs. As an inorganic material, WO_3 has been extensively studied because it has fast response time, intercalation properties (H^+, Li^+, Na^+ and K^+), high coloration efficiency and wavelength selectivity as compared with other inorganic electrochromic materials [9–12]. The

✉ A. Bahari
a.bahari@umz.ac.ir

[1] Department of Mechanical Engineering, West Tehran Branch, Islamic Azad University, Tehran, Iran

[2] Department of Physics, Faculty of Basic Sciences, University of Mazandaran, Babolsar, Iran

[3] Department of Physics, West Tehran Branch, Islamic Azad University, Tehran, Iran

reversible electrochromic effect in the case of WO_3 can be expressed as [13]:

$$WO_3 + xe^- + xM^+ \leftrightarrow M_xWO_3\left(M = H^+, Li^+, Na^+\right) \quad (1)$$

In this process, the electronic structure of WO_3 is modified simultaneously with injection or extraction of electrons and ions and subsequently the Fermi level is moved upwards. As a result of changing of Fermi level, the optical property of WO_3 thin film transforms from a transparent state (Bleached state) to an absorbing one (Colored state). In the composite case when metallic nanoparticles are decorated in the WO_3 matrix, the electrochromic phenomenon can be modified because of a change of the dielectric constant of the oxide matrix [14]. In the last decade, WO_3 composite films containing metal nanoparticles such as Au, Ag and Pt have attracted attention of researchers, which results in the enhancement of coloration efficiency (CE) as well as the durability [15–17]. The electrochromism of metal oxide composite is evaluated in order to enhance the electrochromic properties of pure metal oxide in terms of color tuning via as shift in the absorption band.

In the present work, we synthesized the WO_3 powder as a famous EC metal oxide by sol–gel method and deposited on FTO-coated glass by using the physical vapor deposition (PVD) apparatus. The WO_3–Ag thin film was prepared by deposition of Ag nanoparticles on the surface of WO_3 layer and aneling process. The EC properties of the WO_3–Ag thin film were investigated by cyclic voltammetry (CV) to illustrate reversible color changes and response time. Moreover, the result was compared with WO_3 thin film.

2 Experimental

2.1 Materials

Sodium tungstate ($Na_2WO_4{\cdot}2H_2O$), Ag nanoparticles powder, lithium perchlorate, propylene carbonate (PC), hydrogen peroxide (35%), deionized water (DI), hydrochloric acid, ethanol and acetone were purchased from Merck. The FTO-coated glass was purchased and cut into small pieces with the size of 2×0.9 cm^2.

2.2 Instruments

Deposition of the thin films was done by PVD Apparatus (Meca 2000, France) that equipped with thickness gauge and operated in 10^{-6} torr. CV analyses were done by using the potentiostat/galvanostat Autolab (Nova software model PGSTAT 302N, Metrohm, Netherlands) coupled with a personal computer. CV was measured in 0.5 M $LiClO_4$ in propylene carbonate solution that the FTO-coated glass slide was used as the working electrode and a thin foil of platinum and Ag/AgCl (KCl saturated) were used as counter and reference electrodes, respectively. The FTIR spectra of the samples were measured in the range 400–4000 cm^{-1} by an infrared spectrometer (Bruker, Tensor27 model). The structural characterization of the samples was investigated using a GBC MMA XRD with Cu-Kα radiation (λ = 1.54056 Å) operated at 35 kV in the 2θ range of 5–85 nm with a step of 0.04 nm. The morphology of the thin film was characterized by a field emission scanning electron microscopy (FESEM, model MIRA3 TESCAN, operated at 15 kV) and an atomic force microscopy (AFM, model: AP 0100, Park Scientific Instruments). Element identification results were obtained by energy disperse X-ray spectroscopy (EDX). The optical properties of the films were investigated by UV–Vis spectrophotometer (Shimadzu 210 spectrophotometer).

2.3 Syntheses of WO_3 particles

0.1 M of Sodium tungstate was prepared by dissolving adequate amount of Sodium tungstate in deionized water containing 35% H_2O_2 and was stirred for 20 min at room temperature. The amount of H_2O_2 was set as a molar ratio of 1:4 (W/H_2O_2). Since tungsten oxide (WO_3) synthesis is carried out under acidic conditions and to progress reactions, Nitric acid was added drop wise to adjust the pH value of the solution to 2 [4]. The mixture was kept stirring until a clear pure yellow solution formed. After stirring, a clear pure yellow yields a pale yellow settlement. In the resulting pale yellow yields was filtered, washed with deionized water and dried at 150 °C for 2 h to get WO_3 powder.

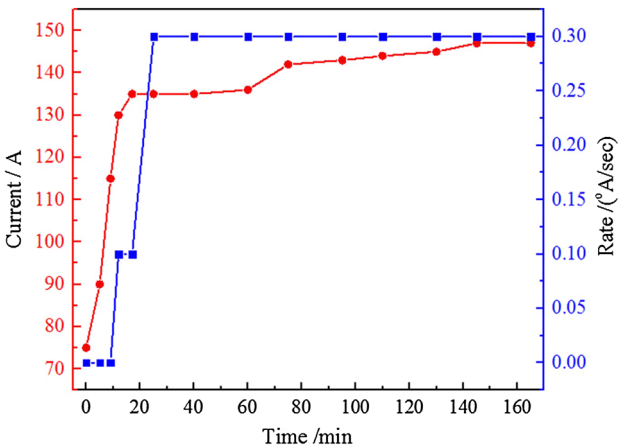

Fig. 1 The *curves* of current and deposition rate versus time in deposition process

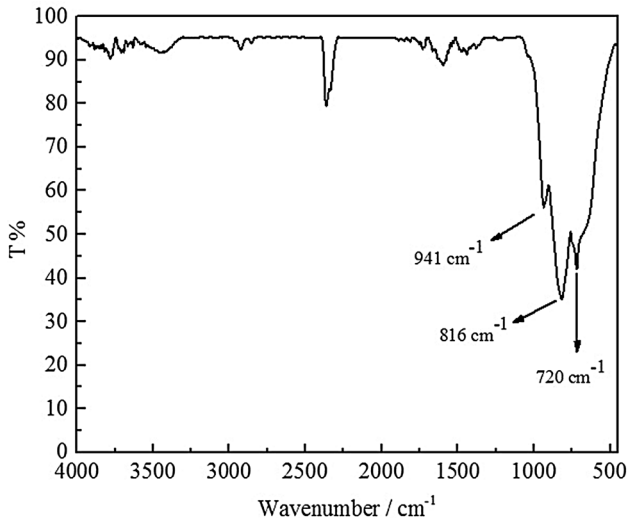

Fig. 2 FTIR spectrum of WO_3 synthesized powder

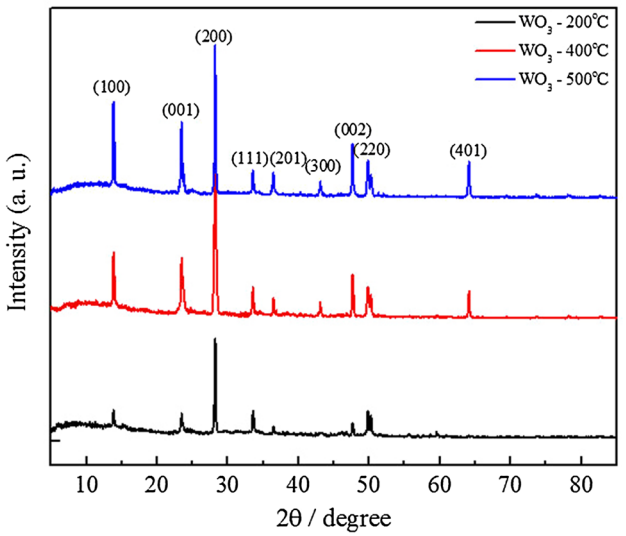

Fig. 3 XRD patterns of WO_3 synthesized powder between 5° and 85° at different annelid temperatures

2.4 Preparation of WO_3–Ag nanocomposite thin film

WO_3 synthesized powder was deposited on the FTO-coated glass substrates (resistance 28–34 Ω/cm^2) using PVD method. Firstly, the FTO-coated glass was cleaned with common detergent and water, HCl 0.1 M, ethanol and finally acetone for 10 min in the ultrasonic bath and at room temperature, respectively. The partial of the FTO was masked as a conducting electrode until during the deposition of WO_3 and Ag powders was protected. Adequate amount of WO_3 powder was added into tungsten boat and due to Fig. 1 by increasing the step by step of current, the rate of deposition was fixed at 0.3 Å/sec. In the deposition process, the thickness and the rate of deposition was monitored by digital thickness display monitor. After the 165 min, the thickness of the film was increased to 315 nm. In the next process, Ag nanoparticles powder as a dopant was used by PVD method. In this process, deposition was continued with deposition rate of 0.1 Å/sec for one minute. The annelid process to crevasse the Ag nanoparticles was applied for 1 min and at 375 °C.

3 Results and discussion

3.1 Structural studies

WO_3 synthesized powder was annelid at 200, 400, 500 °C for 1 h. FTIR spectra of the samples show in Fig. 2. FTIR spectra exhibit characteristic vibrations of WO_3 particles in the range 400–4000 cm^{-1}. The bands at 941, 816 and 720 cm^{-1} are attributed to the O–W–O stretching mode in WO_3 [18–22]. Figure 3 shows the XRD patterns of WO_3 synthesized powder between 5 and 85 nm at different annelid temperatures. All the diffraction peaks indicate the monoclinic phase of WO_3. The mean crystalline size (nm), full with at half maximum of peaks (FWHM) and

Table 1 Information about size, FWHM and integral breadth of XRD major peaks

Peak	300 °C			400 °C			500 °C		
	Size (nm)	FWHM	Integral breadth	Size (nm)	FWHM	Integral breadth	Size (nm)	FWHM	Integral breadth
(100)	11	0.840	1.204	27	0.330	0.524	35	0.253	0.388
(001)	20	0.461	0.706	22	0.410	0.487	33	0.233	0.369
(200)	23	0.210	0.308	27	0.342	0.433	56	0.162	0.243
(111)	33	0.279	0.497	34	0.270	0.426	33	0.282	0.479
(201)	16	1.638	1.299	41	0.227	0.401	39	0.316	0.510
(300)	–	–	–	31	0.304	0.530	39	0.332	0.591
(002)	28	0.349	0.605	37	0.258	0.330	68	0.141	0.245
(220)	24	0.398	0.423	24	0.409	0.462	27	0.648	0.406
(401)	–	–	–	50	0.208	0.315	51	0.203	0.318

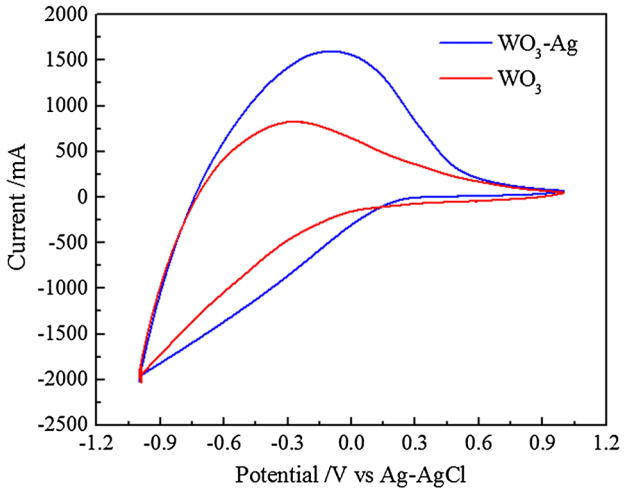

Fig. 4 Cyclic voltammogram of WO_3 (*red line*) and WO_3–Ag (*blue line*) thin films in a 0.5 M solution of $LiClO_4$-PC. (Color figure online)

integral breadth measured using X-powder software based on Scherrer's formula (Eq. 2) reported in Table 1 [23],

$$D = \frac{K\lambda}{\beta\cos\theta} \tag{2}$$

where D is the mean crystalline size, K is the shape factor ($K \approx 0.9$), λ is the wavelength of the X-ray ($\lambda = 1.54056$ Å), θ is Bragg diffraction angle and β is the broadening of the diffraction peak measured at FWHM.

3.2 CV studies

Figure 4 exhibits the CV curves of the WO_3 and WO_3–Ag thin films in 0.5 M $LiClO_4$-PC solution in the potential region from −1.0 to +1.0 V (vs. Ag/AgCl) at scan rate of 50 mV/s. It compares the presence of Ag nanoparticles that are decorated in this method. The WO_3 thin film exhibits the oxidation broad peak at −0.3 V and the reduction broad peak due to the intercalation process of Li^+ into and the deintercalation of Li^+ out from the WO_3 thin film. On the other hand, the WO_3–Ag thin film shows the oxidation broad peak at −0.15 V that is happened farther. Furthermore, the WO_3–Ag thin film has excellent conductivity at positive and negative potentials. It means that the Ag nanoparticles increase the current in this process and it causes better electrochromic inhabitation.

3.3 Morphology studies

The morphologies of the WO_3 and WO_3–Ag thin films are characterized using FESEM and AFM. Figure 3 displays the FESEM and EDX images of WO_3 and WO_3–Ag thin films. It can be seen that the WO_3 thin film is consisted of uniform particles with cleft surface (Fig. 5a). The cleft surface of WO_3 thin film is suitable to penetrate of the other nanomaterials such as Ag nanoparticles into its surface. Figure 5b exhibits the WO_3–Ag thin film. It shows that the structure of the surface is changed after deposition of Ag nanoparticles and annelid process. Figure 6 shows the graph of X-Map of Ag and tungsten nanoparticles on the

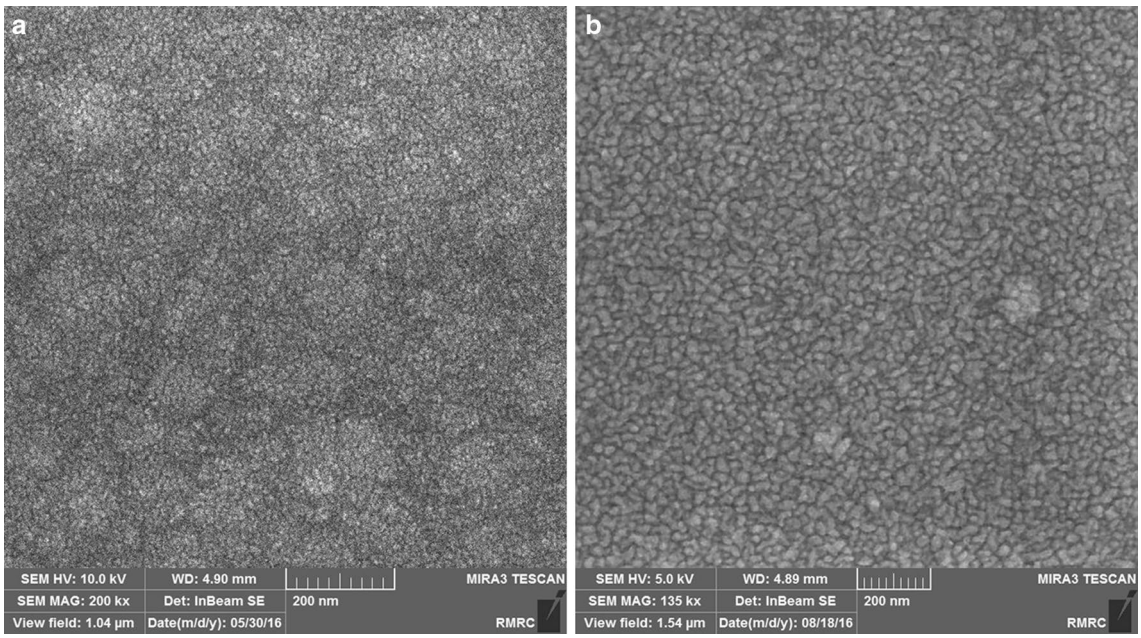

Fig. 5 FESEM images of **a** WO_3 thin film and **b** WO_3–Ag thin film

surface of WO_3–Ag thin film. In these pictures, the sprawl distribution of present particles can be seen on the surface of WO_3–Ag thin film. Figure 7 shows the EDX of different samples which confirm the presence of fundamental elements for each sample. In Fig. 7a, two fundamental elements of WO_3 thin film and in Fig. 7b three fundamental elements of WO_3–Ag thin film can be observed. The weight and atomic percentages of elements in structures of the WO_3 and WO_3–Ag thin films are reported in Table 2.

Figure 8 shows the AFM images of WO_3 and WO_3–Ag thin films. In the Fig. 8a can be seen that the morphology of the WO_3 surface has an approximate roughness about 16 nm and Fig. 8b shows that surface morphology of WO_3–Ag thin film has roughness about 29 nm. These surface morphologies help to electrochromic performance because of the thin film surface can be operated better in beside of electrolyte.

3.4 EC properties

The transmittance of the prepared thin films changes at different applied DC voltage from −1.0 to +1.0 V. The visible transmittance spectra of the WO_3 and WO_3–Ag thin films under different DC voltage were recorded in Fig. 9.

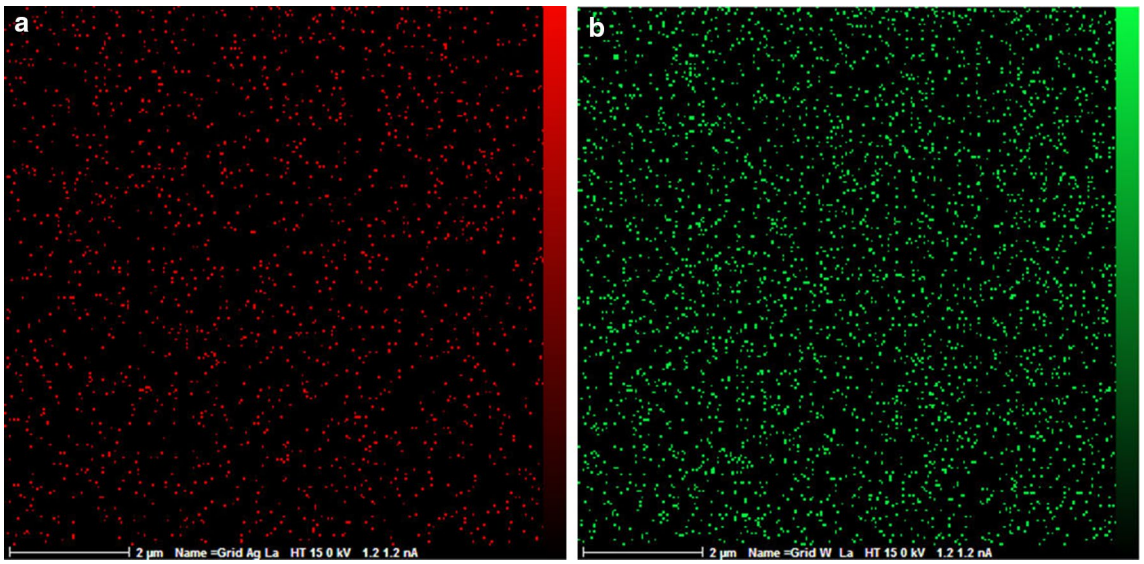

Fig. 6 The X-Map graph of Ag and W nanoparticles on the surface of WO_3–Ag thin film

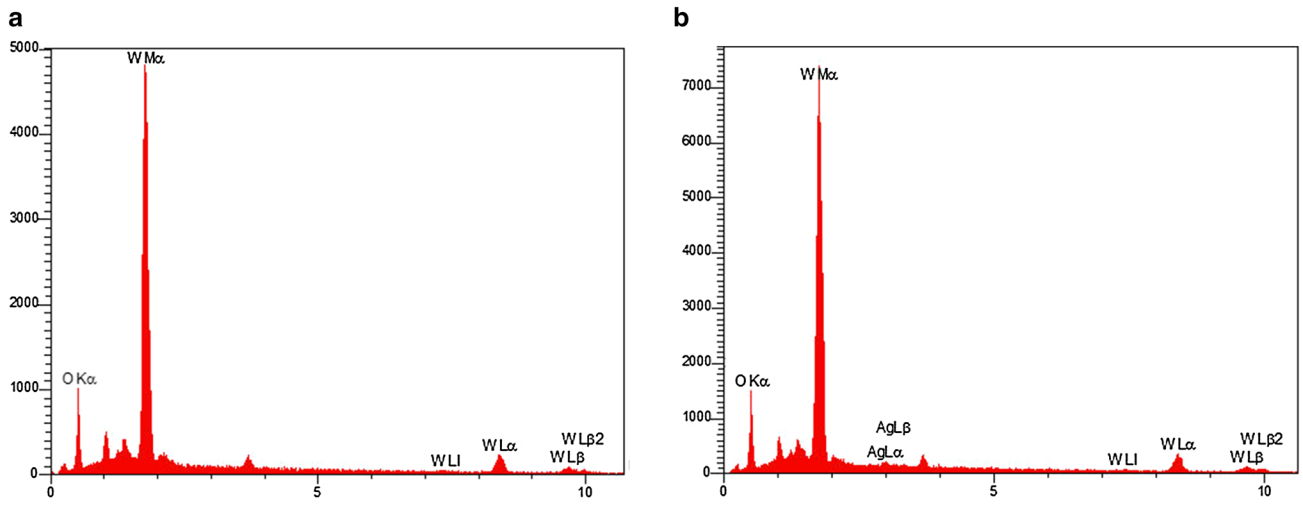

Fig. 7 EDX spectra of the **a** WO_3 and **b** WO_3–Ag thin films

Table 2 The detailed structures of the WO_3 and WO_3–Ag thin films

Sample	Element	W%	A%
WO_3	O	18.07	71.70
	W	81.93	28.30
WO_3–Ag	O	23.42	77.44
	W	73.99	21.29
	Ag	2.59	1.27

Figure 9 shows and compares the visible transmittance spectrum of WO_3 and WO_3–Ag thin films at two applied DC voltages, the first in bleach state at +1.0 V and the second in colored state at −1.0 V. The maximum value of the optical transmittance of the WO_3 thin film in bleached state is 78.93% at 632.8 nm while the minimum value of the optical transmittance in colored state is 43.47% in the same wavelength. So, the difference of transmittance (ΔT %) for WO_3 thin film is equal to 35.46% at 632.8 nm. The visible transmittance of the WO_3–Ag thin film decreases from 80.74 to 41.09% at 632.8 nm when the applied DC voltage decreases from +1.0 to −1.0 V. So, the maximum difference of transmittance for this thin film is equal to 39.65% at 632.8 nm that is higher than the maximum difference of transmittance for WO_3 thin film. These values are reported in Table 3, briefly.

The coloration switching response is a very predominant parameter for EC materials. The switching time is computed as the time required for 90% change in the full transmittance modulation at 632.8 nm. Figures 10 and 11 show the current transient response and corresponding switching curves at 632.8 nm for WO_3 and WO_3–Ag thin films in 0.5 M $LiClO_4$-PC electrolyte. For the WO_3–Ag thin film, the DC voltage steps was applied from −1.0 to +1.0 V and subsequently, the response time for bleached and colored states are calculated as 5.3 and 4.4 s, respectively, which are faster than those of the WO3 thin film (6.9 and 5.3 s). Figure 11 shows the current transient density through the electrochromic film at a consecutive switching in 30 s that it start in about 3 ms for nanocomposite thin film (WO_3–Ag) and it has a sharp drop to zero after the first few seconds. Since 30 s we change voltage from + to − that it makes the current transient density change from + to − and vice versa. Also we can compares the current densities of (WO_3) and (WO_3–Ag) thin films at different sequential switching from +1.0 V to −1.0 and from −1.0 to +1.0 V. As it can be seen, the interchanged charge in WO_3–Ag thin film is less than

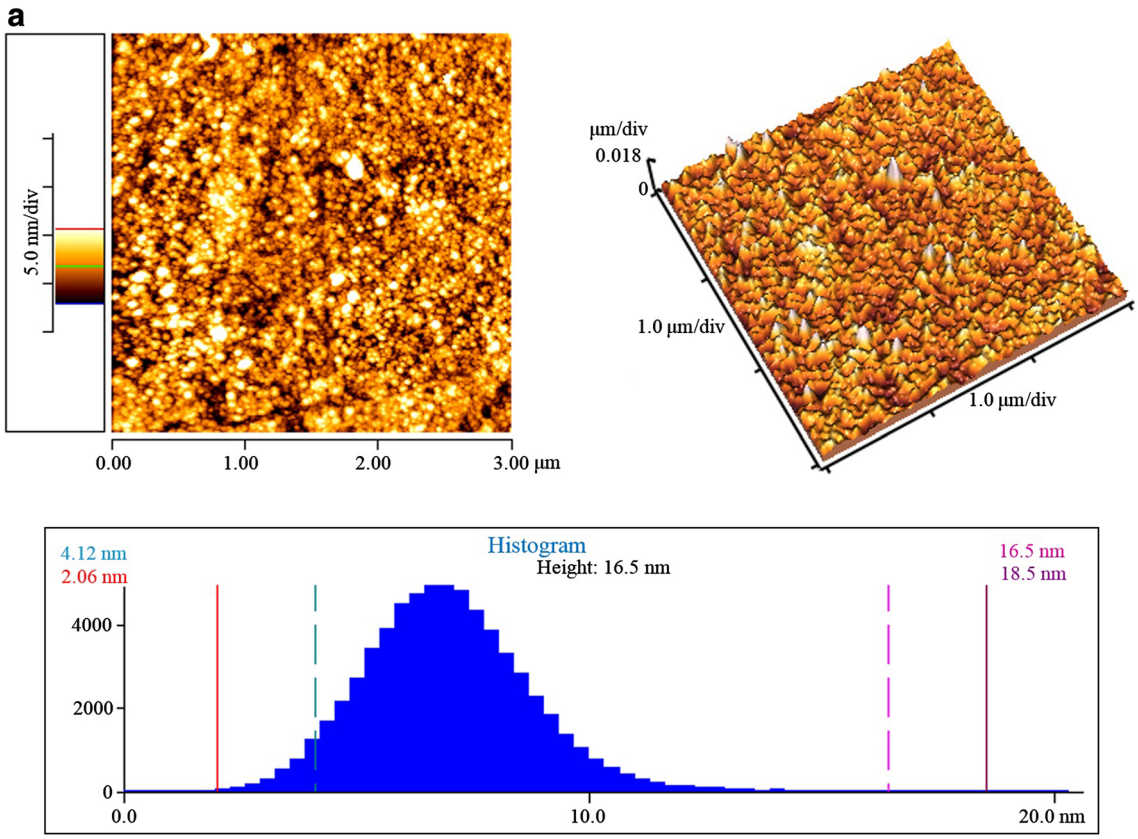

Fig. 8 AFM images of WO_3 and WO_3–Ag thin films. Scan size is 3×3 µm

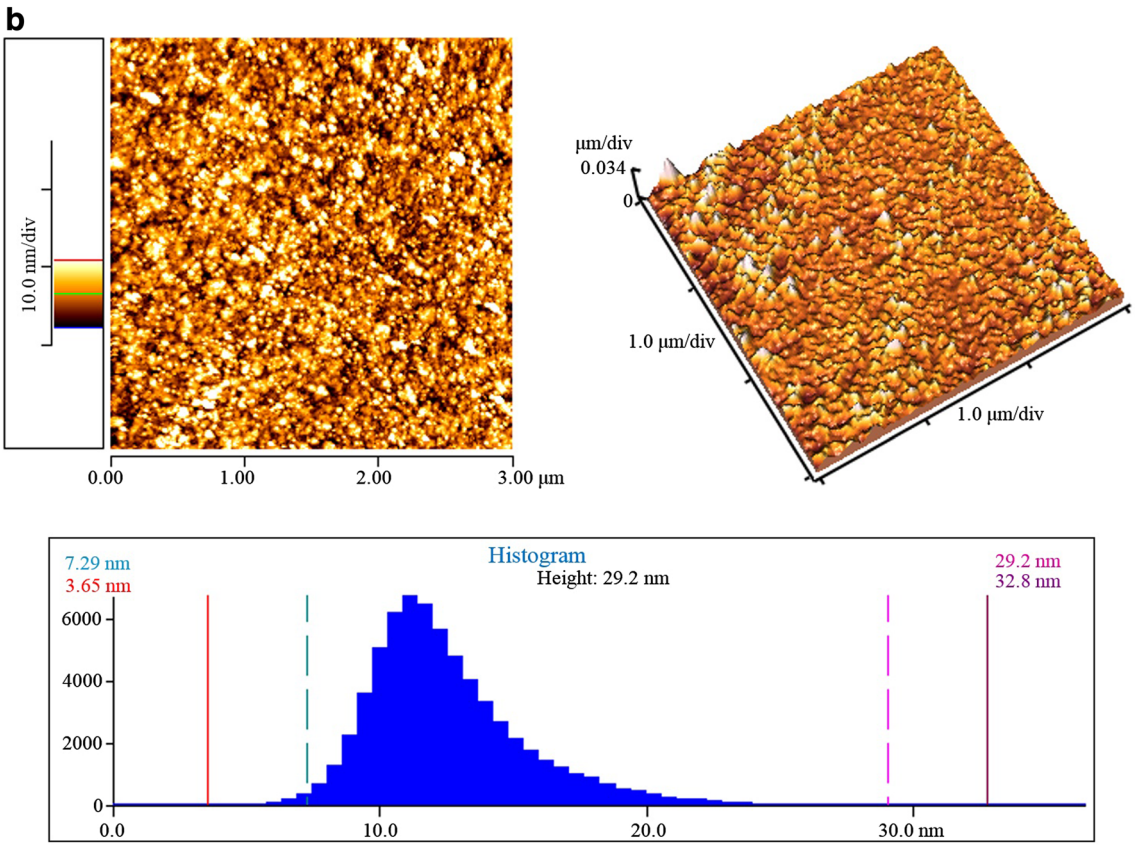

Fig. 8 (continued)

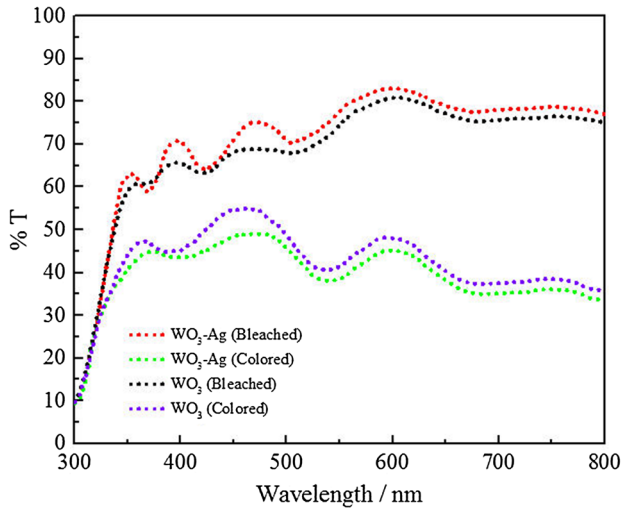

Fig. 9 Visible transmittance spectra of WO_3 and WO_3–Ag thin films under different potentials from −1.0 to +1.0 V

WO_3 thin film. It can be caused that CE of the thin film is enhanced. CE that is important criterion for evaluating EC materials, is extracted from the slope of the change of optical density (ΔOD) between two favorable optical states at a certain wavelength versus corresponding charge density inserted (or extracted) charge density (Q) per unit area (A). It can be investigated according to the Eqs. 3 and 4 [18]:

$$CE = \Delta OD/(Q/A) \tag{3}$$

$$\Delta OD(\lambda) = \log\frac{T_b}{T_c} \tag{4}$$

where T_c and T_b refer to the colored and bleached transmittances of the EC film, respectively. Figure 12 shows the alteration curved of optical density according to the electric charge exchange from the electrolyte to the electrochromic films [24]. Also the slope of the curves demonstrates the amount of CE. As we can see, the plot of ΔOD at 632.8 nm versus the charge density at coloration DC voltage −1.0 V for WO_3 and WO_3–Ag thin films. The CE can be obtained as the slope of the line fitting the linear region of the plot. The CE values of samples are calculated to be 63.5 cm^2/C for WO_3 and 74.2 cm^2/C for WO_3–Ag thin films.

Table 3 Electrochromic properties of WO_3 and WO_3–Ag thin film in 0.5 M solution $LiClO_4$-PC at 632.8 nm

Sample	DC voltage steps/V	T_c/%	T_b/%	ΔT/%	CE/cm^2/C	τ_c/s	τ_B/s
WO_3	+1.0 ↔ −1.0	43.47	78.93	35.46	63.5	5.3	6.9
WO_3-Ag	+1.0 ↔ −1.0	41.09	80.74	39.65	74.2	4.4	5.3

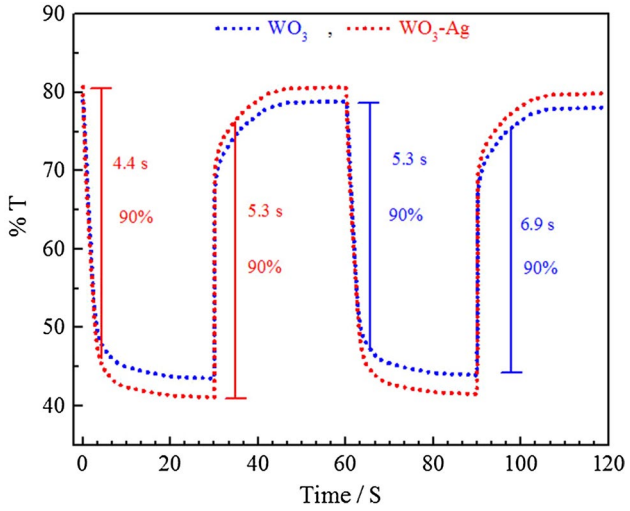

Fig. 10 Electrochromic responses at 632.8 nm for WO_3 thin film (−1.0 to +1.0 V) and WO_3–Ag thin film (−1.0 to +1.0 V) in 0.5 M $LiClO_4$-PC electrolyte

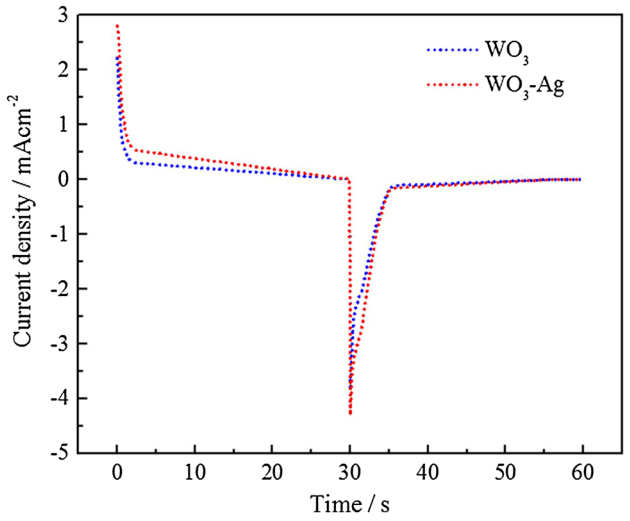

Fig. 11 The current curves versus time for WO_3 thin film (−1.0 to +1.0 V) and WO_3–Ag thin film (−1.0 to +1.0 V) in 0.5 M $LiClO_4$-PC electrolyte

4 Conclusions

The WO_3 particles have been successfully synthesized with sol–gel method that crystalline size were estimated from

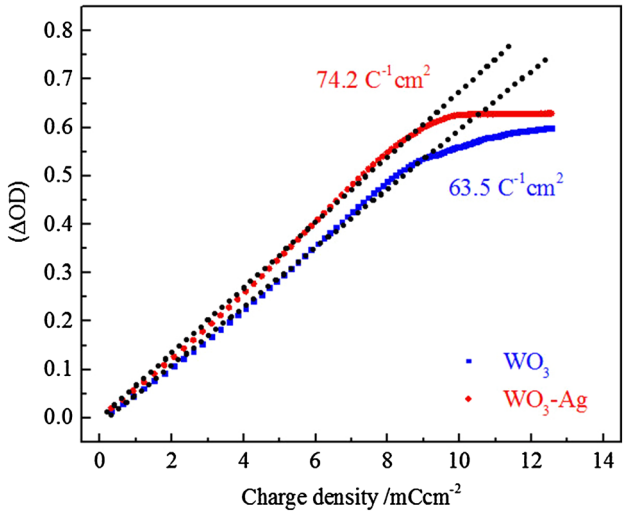

Fig. 12 Variation of the in situ optical density (OD) versus charge density for WO_3 thin film and WO_3–Ag thin film

XRD which all the diffraction peaks indicate the monoclinic structure phase of WO_3 and it deposited on FTO-coated glass substrate by PVD method. The WO_3–Ag nanocomposite has been deposited on FTO by PVD method and compered with pure WO_3 thin film in EC properties. FESEM shows, thin films are consisted of uniform particles and EDX images confirm the presence of fundamental elements for each sample. CV result shows the Ag nanoparticles increase the current and it causes better EC inhabitation. AFM confirms surface morphologies that WO_3–Ag nanocomposite can be operated better in beside of electrolyte. In the other hand, the composition of Ag nanoparticles has improved some advantages and properties to the EC film. First, the change of transmittance of WO_3–Ag nanocomposite thin film at 632.8 nm has increased to 40.59% at DC voltage steps −1.0 to +1.0 V in 0.5 M $LiClO_4$-PC solution. Second, the response time of WO_3–Ag thin film for bleached states has decreased from 11 to 8.9 s and for colored states decreased from 4.2 to 3.9 s at same DC voltage steps. Third, the CE of WO_3–Ag nanocomposite thin film at 632.8 nm increases to 74.2 cm^2/C. At the end, we can find out that, In this experimental work, we improve three important applied EC's properties by dopant of Ag nanoparticles on surface of WO_3 thin film: (change of transmittance) that optimize 4–5%, (coloration efficiency) that enhance 10.7 cm^2/C and (switching response) for both bleached and colored positions were amended.

References

1. C.G. Granqvist, Electrochromics for smart windows: oxide-based thin films and devices. Thin Solid Films **564**, 1–38 (2014)
2. Y. Zhao, R. Xu, X. Zhang, X. Hu, R.J. Knize, Y. Lu, Simulation of smart windows in the ZnO/VO_2/ZnS sandwiched structure with improved thermochromic properties. Energy Build. **66**, 545–552 (2013)
3. H. Li, Y. Lv, X. Zhang, X. Wang, X. Liu, High-performance ITO-free electrochromic films based on bi-functional-stackedWO_3/Ag/WO_3 structures. Sol. Energy Mater. Sol. Cells **136**, 86–91 (2015)
4. H. Najafi-Ashtiani, A. Bahar, S. Ghasemi, A dual electrochromic film based on nanocomposite of copolymer and WO3 nanoparticles: Enhanced electrochromic coloration efficiency and switching response. J. Electroanal. Chem. **774**, 14–21 (2016)
5. N. Naseri, R. Azimirad, O. Akhavan, A.Z. Moshfegh, Improved electrochromical properties of sol–gel WO_3 thin films by doping gold nanocrystals. Thin Solid Films **518**, 2250–2257 (2010)
6. C.G. Granqvist, *Handbook of inorganic electrochromic materials*. (Elsevier, Amsterdam, 1995)
7. Y. Pang, Q. Chen, X. Shen, L. Tang, H. Qian, Size-controlled Ag nanoparticle modified WO_3 composite films for adjustment of electrochromic properties. Thin Solid Films **518**, 1920–1924 (2010)
8. Q. Tang, L. He, Y. Yang, J. Long, X. Fu, C. Gong, Effects of substitution position on electrochemical, electrochromic, optical, and photoresponsive properties of azobenzenecarboxylic acid alkyl ester derivatives. Org. Electron. **30**, 200–206 (2016)
9. Y.S. Krasnov, G.Y. Kolbasov, Electrochromism and reversible changes in the position of fundamental absorption edge in cathodically deposited amorphous WO_3. Electrochim. Acta **49**, 2425–2433 (2004)
10. A. Subrahmanyam, A. Karuppasamy, Optical and electrochromic properties of oxygen sputtered tungsten oxide (WO_3) thin films. Sol. Energy Mater. Sol. Cells **91**, 266–274 (2007)
11. K. Sauvet, L. Sauques, A. Rougier, IR electrochromic WO_3 thin films: from optimization to devices. Sol. Energy Mater. Sol. Cells **93**, 2045–2049 (2009)
12. S. Park, S. Kim, J. Choi, J. Song, M. Taya, S. Ahn, Low-cost fabrication of WO_3 films using a room temperature and low-vacuum air-spray based deposition system for inorganic electrochromic device applications. Thin Solid Films **589**, 412–418 (2015)
13. E. Koubli, S. Tsakanikas, G. Leftheriotis, G. Syrrokostas, P. Yianoulis, Optical properties and stability of near-optimumWO_3/Ag/WO_3 multilayers for electrochromic applications. Solid State Ionics **272**, 30–38 (2015)
14. K.-W. Park, Electrochromic properties of Au–WO_3 nanocomposite thin-film electrode. Electrochim. Acta **50**, 4690–4693 (2005)
15. K.-W. Park, H.-S. Shim, T.-Y. Seong, Y.-E. Sung, Modified electrochromism of tungsten oxide via platinum nanophases. Appl. Phys. Lett. **88**, 211107 (2006)
16. D.R. Acosta, C. Magaña, F. Hernández, J. Ortega, Electrical, optical and electrochromic properties of Ti:WO_3 thin films deposited by the pulsed chemical spray technique. Thin Solid Films **594**, 207–214 (2015)
17. I. Porqueras, E. Bertran, Optical properties of Li doped electrochromic WO_3 thin films. Thin Solid Films **377–378**, 8–13 (2000)
18. G.F. Cai, J.P. Tu, D. Zhou, J.H. Zhang, X.L. Wang, C.D. Gu, Dual electrochromic film based on WO_3/polyaniline core/shell nanowire array. Sol. Energy Mater. Sol. Cells **122**, 51–58 (2014)
19. S. Badilescu, P.V. Ashrit, Study of sol–gel prepared nanostructured WO_3 thin films and composites for electrochromic applications. Solid State Ionics **158**, 187–197 (2003)
20. A.A. El-Kheshen, F.H. El-Batal, UV-visible, infrared and Raman spectroscopic and thermal studies of tungsten doped lead borate glasses and the effect of ionizing gamma irradiation. Indian J. Pure Appl. Phys. **46**, 225–238 (2008)
21. N. Parvatikar, S. Jain, S. Khasim, M. Revansid, S.V. Bhoraskar, M.V.N. Ambika Prasad, Electrical and humidity sensing properties of polyaniline/WO_3 composites. Sens Actuators B **114**, 599–603 (2006)
22. F. Mehmood, J. Iqbal, T. Jan, W. Ahmed, W. Ahmed, A. Arshad, Q. Mansoor, S.Z. Ilyas, M. Ismail, I. Ahmad, Effect of Sn doping on the structural, optical, electrical and anticancer properties of WO_3 nanoplates. Ceram. Int. **42**, 14334–14341 (2016)
23. J. Zhang, J.P. Tu, D. Zhang, Y.Q. Qiao, X.H. Xia, X.L. Wang, C.D. Gu, Multicolor electrochromic polyaniline-WO_3 hibrid thin film: one-pot molecular assembling synthesis. J. Mater. Chem. **21**, 17316–17324 (2011)
24. H. Najafi-Ashtiani, A. Bahari, S. Ghasemi, A dual electrochromic film based on nanocomposite of aniline and o-toluidine copolymer with tungsten oxide nanoparticles. Org. Electron. **37**, 213–221 (2016)